LETTERS
PUBLISHED ONLINE: 5 FEBRUARY 2012 | DOI: 10.1038/NCLIMATE1385

nature climate change

Global warming under old and new scenarios using IPCC climate sensitivity range estimates

Joeri Rogelj[1]*, Malte Meinshausen[2,3] and Reto Knutti[1]

Climate projections for the fourth assessment report[1] (AR4) of the Intergovernmental Panel on Climate Change (IPCC) were based on scenarios from the *Special Report on Emissions Scenarios*[2] (SRES) and simulations of the third phase of the Coupled Model Intercomparison Project[3] (CMIP3). Since then, a new set of four scenarios (the representative concentration pathways or RCPs) was designed[4]. Climate projections in the IPCC fifth assessment report (AR5) will be based on the fifth phase of the Coupled Model Intercomparison Project[5] (CMIP5), which incorporates the latest versions of climate models and focuses on RCPs. This implies that by AR5 both models and scenarios will have changed, making a comparison with earlier literature challenging. To facilitate this comparison, we provide probabilistic climate projections of both SRES scenarios and RCPs in a single consistent framework. These estimates are based on a model set-up that probabilistically takes into account the overall consensus understanding of climate sensitivity uncertainty, synthesizes the understanding of climate system and carbon-cycle behaviour, and is at the same time constrained by the observed historical warming.

A thorough comparison of SRES scenarios and RCPs would ideally be based on results computed by the exact same set of models. Running the new RCPs with the full suite of CMIP3 atmosphere–ocean general circulation models (AOGCM) is unrealistic because many models are now obsolete or unmaintained, and also because the computational cost is prohibitive. The latter restriction also applies to running all SRES scenarios with present versions of AOGCMs. We therefore use a reduced-complexity carbon-cycle and climate model MAGICC (ref. 6) version 6 to compare SRES scenarios and RCPs. The MAGICC model closely emulates[7] the global and annual mean behaviour of significantly more complex AOGCM and C^{4}MIP carbon-cycle models. We use historical constraints and calculate probabilistic time-evolving temperature projections for both sets of scenarios (see Methods). We derive a climate sensitivity distribution starting from the overall consensus understanding of climate sensitivity uncertainties—and then re-sample the joint distribution of climate model parameters such that historically observed ocean's surface and land's air temperatures in both hemispheres[8], as well as ocean heat uptake observations[9], are matched. The resulting model set-up closely reflects the uncertainties in radiative forcing, carbon-cycle and climate sensitivity from the AR4 (see Methods and ref. 10).

Equilibrium climate sensitivity (ECS)—the change in global mean surface temperature at equilibrium following a doubling of atmospheric carbon dioxide (CO_2) concentrations—remains a critical source of uncertainty in long-term temperature projections[1]. It is not a physical quantity that can be measured directly through observations, but can be estimated with different indirect methods (see ref. 11 and references therein). The IPCC AR4 concludes[1] that ECS is likely (greater than 66% probability[12]) in the range from 2 to 4.5 °C, with a most likely value (mode) of about 3 °C. Furthermore, ECS is very likely (greater than 90% probability[12]) larger than 1.5 °C, and values substantially higher than 4.5 °C cannot be excluded. These values seem now to be rather robust estimates as they have not changed much for almost two decades (Table 1) and more recent studies have supported these estimates[13–15]. The concluding statements of the IPCC AR4 synthesize the literature but no probability density function (PDF) was provided. For our probabilistic model framework we require such a distribution and thus apply a methodology that aims at incorporating the IPCC AR4 synthesizing statements transparently into one distribution. This necessarily requires additional assumptions beyond AR4 (see Supplementary Table S1), which are partly subjective but do not strongly affect the results. In fact, our main result, the quantitative analysis of the differences between RCPs and SRES, is hardly affected at all, which we tested by assuming alternative ECS distributions from the literature (see Supplementary Table S2). Our methodology translates the AR4 consensus understanding on climate sensitivity uncertainty into a PDF, noting that this still relies on an initial expert assessment of the multiple lines of evidence. A methodology to formally combine climate sensitivity estimates from different lines of evidence will remain a challenge, as the various estimates are not fully statistically independent[11]. In our interpretation of the AR4 ECS assessment we follow the guidelines of the IPCC (refs 12,16) on the interpretation of likelihood ranges, but note that also other interpretations exist in the literature[17].

Earlier studies have used different analytical forms to generate a PDF from IPCC statements (for example, see ref. 18). We apply a more generalized approach and create an ensemble of ten thousand distributions (Fig. 1 and Methods) that all comply with these AR4 synthesizing statements and of which the spread spans the range that is left open by the IPCC AR4 assessment (Fig. 1). A representative distribution is computed by taking the arithmetic mean over all ten thousand distributions. The computed distribution by design complies with the AR4 ranges (Table 1) and the shape lies within the range found in the literature[11]. Our average ECS distribution represents a mean result over ten thousand possible outcomes, and is hence neither the most conservative nor the most optimistic interpretation of the IPCC AR4 ECS statements. ECS values in our average distribution are higher than 1.5 °C with 95% probability, fall between 2 and 4.5 °C with 76% probability and exceed 4.5 °C with 14% probability (Table 1). The most likely value (mode) of our distribution is at 3 °C. The exact shape is irrelevant for our core conclusions. Of importance is that the same model and parameters are used to compare SRES scenarios and RCPs.

[1]Institute for Atmospheric and Climate Science, ETH Zurich, Universitätstrasse 16, 8092 Zürich, Switzerland, [2]PRIMAP Group, Earth System Analysis, Potsdam Institute for Climate Impact Research (PIK), PO Box 60 12 03, 14412 Potsdam, Germany, [3]School of Earth Sciences, University of Melbourne, Victoria 3010, Australia. *e-mail: joeri.rogelj@env.ethz.ch.

© 2012 Macmillan Publishers Limited. All rights reserved.

Table 1 | Key characteristics of illustrative Bayesian ECS distributions from the literature (non-exhaustive), and from this study's representative ECS distribution and 10,000-member ECS ensemble.

Study	Probability			Most likely value
	Above 1.5 °C	Between 2.0 °C and 4.5 °C	Above 4.5 °C	
Illustrative individual studies (non-exhaustive)				
Hegerl *et al.*[33]	87%	44%	34%	2.0 °C
Forster *et al.*[34]	82%	46%	20%	1.6 °C
Annan and Hargreaves[35]	98%	88%	5%	2.9 °C
Forest *et al.*[36] ('no expert priors' case)	100%	90%	6%	2.8 °C
Knutti *et al.*[37]	95%	71%	20%	3.2 °C
Murphy *et al.*[38]	100%	86%	14%	3.2 °C
Piani *et al.*[39]	99%	72%	24%	3.2 °C
Frame *et al.*[40]	100%	85%	12%	2.8 °C
Multiple lines of evidence				
IPCC FAR[41], SAR[42], TAR[43]	-	1.5–4.5 °C (no probability)	-	-
IPCC AR4 (ref. 1)	> 90%	> 66%	Not excluded	About 3 °C
This study's representative climate sensitivity distribution	95%	76%	14%	3.0 °C
Minimum–maximum values in this study's 10,000-member ECS ensemble	90 to > 99%	66–96%	< 1–33%	2.6–3.6 °C

Note that the studies listed are only a small selection of the Bayesian ECS distributions shown in Fig. 1, are not all independent and present only a small subset of studies that informed the IPCC AR4 conclusions on ECS, which were taken on the basis of multiple lines of evidence[11]. Also note that the different studies use different prior distributions for climate sensitivity[44]. More details are provided in Supplementary Table S4.

A deeper level of uncertainty in the ECS distribution exists and is illustrated by the envelope of all possible ECS distributions in line with the AR4 ECS synthesis assessment. We have quantified this uncertainty by means of a sensitivity analysis of our results for the RCPs with a selection of four ECS distributions. These four distributions represent extremes within our 10,000-member ECS distribution ensemble. We selected the ECS with the highest cumulative probability below 1.5 °C, with the highest cumulative probability above 4.5 °C, and with the highest and the lowest temperature difference between the 17 and 83% cumulative probabilities (that is, a very broad and a very narrow distribution), respectively.

A straightforward application of the computed ECS distribution is to link it to atmospheric greenhouse-gas (GHG) concentrations in a probabilistic way, as proposed previously[19]. Other examples are analyses regarding the relationship between GHG concentrations and 2 °C (ref. 20) and Table 10.8 of the AR4 (ref. 21). The latter links equilibrium temperature increase to the CO_2 concentration level equivalent to the net radiative forcing at equilibrium from all forcing agents. It therefore takes into account the contributions of both short- (for example, soot or other aerosols) and long-lived species. For an equivalent CO_2 concentration of 450 parts per million CO_2 equivalent (ppm CO_2e), Table 10.8 of the AR4 gives a best-guess temperature increase above pre-industrial at equilibrium of 2.1 °C ('very likely' or with greater than 90% probability[12] above 1.0 °C, and 'likely' or with greater than 66% probability[12] in the range 1.4 to 3.1 °C). In our results, a 450 ppm CO_2e concentration level is consistent with a probability of 60% to exceed 2 °C temperature increase at equilibrium (Fig. 2) with a minimum–maximum range of 57–89% over our four sensitivity cases (see earlier). Likewise, limiting the global temperature increase at equilibrium to 2 °C (1.5 °C) above pre-industrial levels with a 'likely' (greater than 66%) chance would require stabilization of equivalent atmospheric CO_2 concentrations from all forcing agents at less than 415 (370) ppm CO_2e. On the basis of our four sensitivity cases of ECS distributions, we find ranges of 380–420 ppm CO_2e for 2 °C, and 350–375 ppm CO_2e for 1.5 °C. The ability to draw such links in a simple, transparent way that is consistent with a consensus assessment of ECS is becoming more important with international climate policy starting to focus on temperature limits (such as the 1.5 and 2 °C limits mentioned in the Cancūn Agreements[22] and in the outcome of the Durban climate change conference).

With a representative ECS distribution at hand, the core question of this paper can be analysed. Therefore, we first compute temperature projections for the six SRES marker scenarios. Our median temperature estimates (Fig. 3 and Table 2) are by definition different from the 'best estimate' temperature projections in the AR4 that were defined as the mean over all CMIP3 AOGCM model projections[23]. The mean absolute difference between our median projections and the AR4 'best estimate' is however small (less than 0.07 °C).

For the 'likely' (greater than 66% probability[12]) ranges of the temperature projections in the IPCC AR4, a −40 to +60% range around the multi-model mean was given[23]. This range was developed on the basis of expert judgement and all available estimates[23]. Our results for the 90% uncertainty range are close to the above-mentioned 'likely' AR4 range (Fig. 3b and Table 2). This contraction of the uncertainty ranges in our results is due to the fact that we use an average ECS distribution and a single consistent probabilistic modelling framework for our projections. Structural model uncertainty in the energy-balance approach is not considered. In addition, our approach assumes the range of carbon-cycle/climate feedbacks in C^4MIP to be representative of the full uncertainties. Although this is plausible, IPCC assessments try to additionally account for uncertainties that may not be fully sampled by the ensembles of opportunities[24], and attempt to include structural model uncertainty and uncertainty in methodological frameworks. As our approach does not do so, the contraction of the uncertainty ranges in our results should not be seen as an improvement or correction of the IPCC assessment. Rather, the strength of our results lies in the fact that they provide comparison data for the SRES scenarios and RCPs derived from one single probabilistic framework that is closely in line with the IPCC AR4 assessment.

© 2012 Macmillan Publishers Limited. All rights reserved.

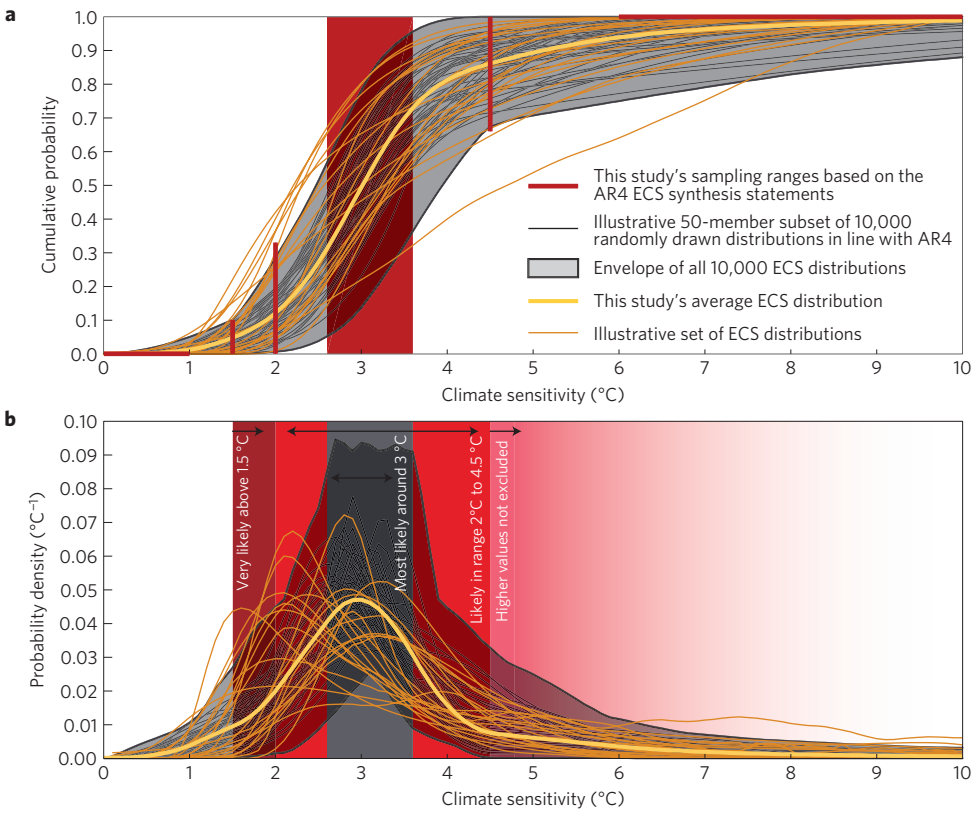

Figure 1 | Ensemble of ECS distributions from this study and from the literature. a, Cumulative distribution functions of ECS. Thick red lines and areas indicate sample ranges for start, end and intermediary points of the cumulative distribution functions based on the IPCC AR4 ECS synthesizing statements. The shaded grey area bounded by a thick black line represents the envelope of all 10,000 randomly drawn ECS distributions (thin black lines) that are in line with these AR4 ECS statements. Thin orange lines are illustrative Bayesian ECS distributions[14,18,33–39,44–48] (more details are provided in Supplementary Table S4). Note that not all curves of this illustrative set are equally credible and that the IPCC synthesizing statements were based on additional lines of evidence, some of them tending to suggest a higher most likely value compared with the illustrative set of Bayesian literature PDFs shown here. The thick yellow line is this study's representative distribution based on the IPCC AR4 ECS synthesizing statements. **b**, Corresponding PDFs. Note that although the horizontal axis is truncated at 10 °C, the randomly drawn distributions were not constrained to values below 10 °C.

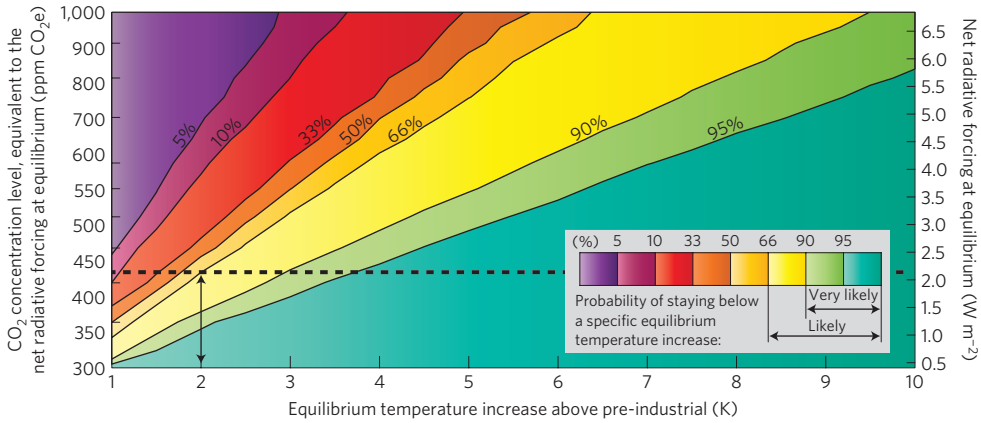

Figure 2 | Probability to stay below specific equilibrium temperature increases relative to pre-industrial as a function of equivalent atmospheric CO_2 concentration stabilization levels based on this study's representative ECS distribution. Note that the left scale indicates the CO_2 concentration level, equivalent to the net radiative forcing at equilibrium resulting from all forcing agents. It includes both the contributions of short- (for example, soot and aerosols) and long-lived (for example, CO_2) forcing agents. The right scale directly shows the equivalent net radiative forcing. The arrow illustrates that to limit global temperature increase to below 2 °C with a 'likely' (greater than 66%) probability, equivalent CO_2 concentrations at equilibrium should be lower than 415 ppm CO_2e or the net radiative forcing at equilibrium below about 2.1 W m^{-2}.

Finally, we estimate what temperature increase the RCPs (ref. 25) would have yielded on the basis of two different methods: emission- and concentration-driven. The emission-driven modelling results are comparable to the SRES results, and the Earth-system-model-driven RCP experiments in CMIP5, whereas the concentration-driven model runs allow for a better comparability to most CMIP5 experiments, in which AOGCMs prescribe atmospheric concentration levels for CO_2, CH_4, N_2O and

© 2012 Macmillan Publishers Limited. All rights reserved.

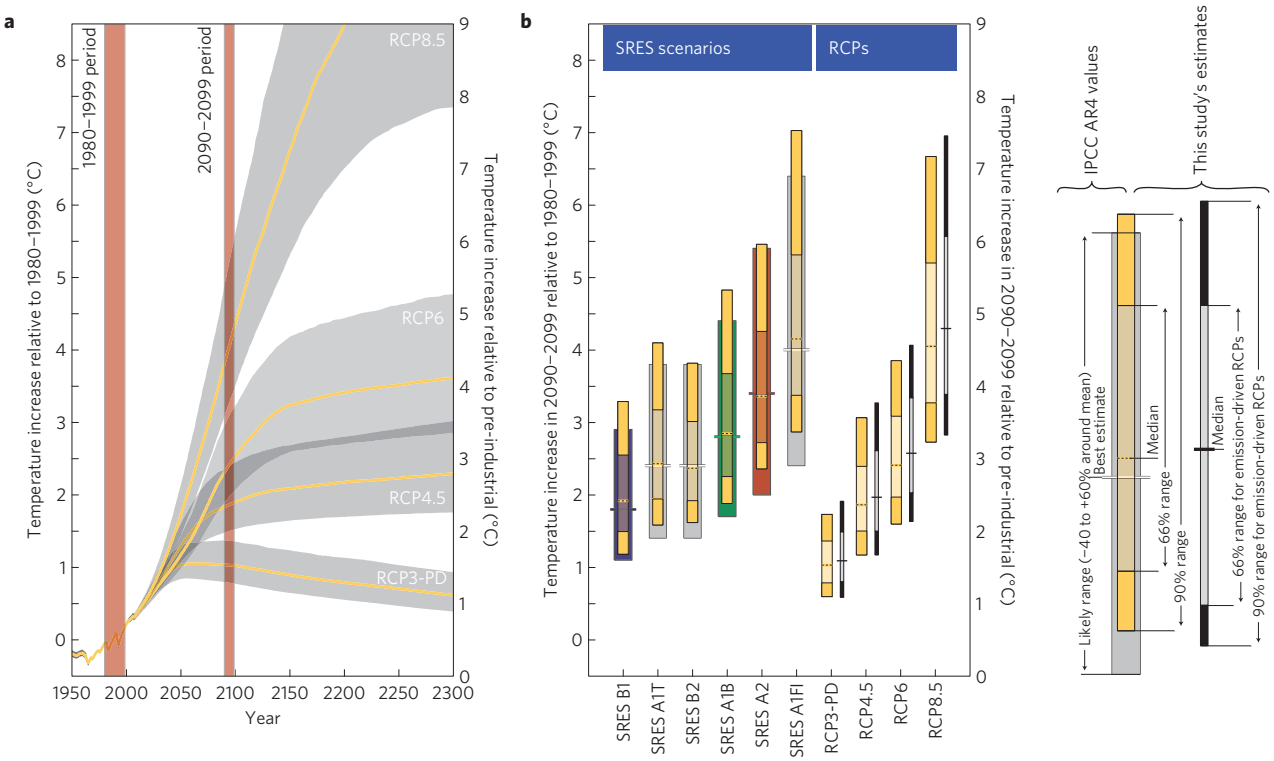

Figure 3 | Temperature projections for SRES scenarios and RCPs. a, Time-evolving temperature distributions (66% range) for the four concentration-driven RCPs computed with this study's representative ECS distribution and a model set-up representing closely the climate system uncertainty estimates of the AR4 (grey areas). Median paths are drawn in yellow. Red shaded areas indicate time periods referred to in **b**. **b**, Ranges of estimated average temperature increase between 2090 and 2099 for SRES scenarios and RCPs respectively. Note that results are given both relative to 1980–1999 (left scale) and relative to pre-industrial (right scale). Yellow and thin black ranges indicate results of this study; other ranges show the AR4 estimates (see legend at right-hand side). Colour-coding of AR4 ranges is chosen to be consistent with the AR4 (see Figure SPM.5 in ref. 1). For RCPs, yellow ranges show concentration-driven results, whereas black ranges show emission-driven results.

Table 2 | Probabilistic estimates of temperature increase above pre-industrial levels based on this study's representative ECS distribution for the six SRES marker scenarios and the four RCPs.

	Temperature increase above pre-industrial (°C)					
Scenario	**2090–2099 period**		**2100**		**2300**	
IPCC AR4	Best estimate	Likely range	Median	66% range	Median	66% range
SRES B1	2.3	1.6–3.4	-	-	-	-
SRES A1T	2.9	1.9–4.3	-	-	-	-
SRES B2	2.9	1.9–4.3	-	-	-	-
SRES A1B	3.2	2.2–4.9	-	-	-	-
SRES A2	3.9	2.5–5.9	-	-	-	-
SRES A1FI	4.5	2.9–6.9	-	-	-	-
This study	Median	66% range	Median	66% range	Median	66% range
SRES B1	2.4	2.0–3.1	2.5	2.0–3.2	-	-
SRES A1T	2.9	2.5–3.7	3.0	2.5–3.8	-	-
SRES B2	2.9	2.4–3.5	3.0	2.6–3.7	-	-
SRES A1B	3.4	2.8–4.2	3.5	2.9–4.4	-	-
SRES A2	3.9	3.2–4.8	4.2	3.5–5.2	-	-
SRES A1FI	4.7	3.9–5.8	5.0	4.1–6.2	-	-
RCP3-PD	1.5	1.3–1.9	1.5	1.3–1.9	1.1	0.9–1.5
RCP4.5	2.4	2.0–2.9	2.4	2.0–3.0	2.8	2.3–3.5
RCP6	2.9	2.5–3.6	3.0	2.6–3.7	4.1	3.4–5.3
RCP8.5	4.6	3.8–5.7	4.9	4.0–6.1	10.0	7.9–14.1

Note that estimates in AR4 were given relative to 1980–1999. The 'likely range' denotes the 'greater than 66%' probability range as suggested by the IPCC (ref. 12). The '66% range' labels denote the 66% range as such. RCP results are from concentration-driven runs. Results for emission-driven RCP runs are provided in Supplementary Table S3.

© 2012 Macmillan Publishers Limited. All rights reserved.

Table 3 | Main similarities and differences between temperature projections for SRES scenarios and RCPs.

RCP	SRES scenario with similar median temperature increase by 2100	Particular differences
RCP3-PD	None	The ratio between temperature increase and net radiative forcing in 2100 is 0.88 °C $(W\,m^{-2})^{-1}$ for RCP3-PD, whereas all other scenarios show a ratio of about 0.62 °C $(W\,m^{-2})^{-1}$; that is, RCP3-PD is closer to equilibrium in 2100 than the other scenarios.
RCP4.5	SRES B1	Median temperatures in RCP4.5 rise faster than in SRES B1 until mid-century, and slower afterwards.
RCP6	SRES B2	Median temperatures in RCP6 rise faster than in SRES B2 during the three decades between 2060 and 2090, and slower during other periods of the twenty-first century.
RCP8.5	SRES A1FI	Median temperatures in RCP8.5 rise slower than in SRES A1FI during the period between 2035 and 2080, and faster during other periods of the twenty-first century.

See also Supplementary Fig. S2.

other GHGs. The concentration-driven and emission-driven estimates provide a proxy for RCP results from the previous CMIP3 intercomparison and C^4MIP intercomparison, respectively (see ref. 7). Here we present the concentration-driven results (Fig. 3 and Table 2). For comparison, the emission-driven results are also given in Fig. 3b and Supplementary Table S3.

The RCPs span a large range of stabilization, mitigation and non-mitigation pathways. The resulting range of temperature estimates is therefore larger than the range of the SRES scenarios, which cover only non-mitigation scenarios (Table 2). RCP8.5, representing a high-emission, non-mitigation future, yields a range of temperature outcomes of 4.0 to 6.1 °C by 2100 (66% range). The lowest RCP (ref. 26), assuming significant climate action, limits global temperature increase to below 2 °C with a 'likely' chance (greater than 66% probability). The latter result is hence also consistent with some AOGCMs yielding temperature projections that will exceed 2 °C for the lowest RCP. On the basis of our four sensitivity ECS distributions, we find that the 66 (90)% uncertainty ranges for the temperature projections for the RCPs in 2100 (as reported in Table 2 on the basis of our average ECS distribution) can be up to 13 (41)% wider or up to 38 (41)% narrower when using one of these four extreme ECS distributions from our set (see Supplementary Fig. S1).

Although the RCPs were not developed to mimic specific SRES scenarios, pairs with similar temperature projections over the twenty-first century can be found between the two sets (see also Tables 2 and 3 and Fig. 3). The highest RCP (ref. 27) would yield temperature projections close to those of the SRES A1FI scenario. RCP6 temperature projections are similar to those of SRES B2 and, likewise, RCP4.5 temperature projections to those of SRES B1.

Global mean temperature projections by the end of the twenty-first century for the RCPs are very similar to those of their closest SRES counterparts (Table 2). However, the transient trajectories differ in various ways (Table 3 and Supplementary Fig. S2). These different warming rates between SRES scenarios and RCPs with similar year 2100 forcing are due to different transient forcings up to then. These differences can be of importance when assessing shorter-term climate impacts under RCPs and comparing them to earlier literature.

All SRES scenarios are non-intervention scenarios with an increasing forcing path during the twenty-first century. The new, lowest RCP scenario[26] is fundamentally different from these. Its radiative forcing peaks during the twenty-first century at around 3 $W\,m^{-2}$ and declines afterwards. Our probabilistic results show distinct characteristics for RCP3-PD, which will have to be validated once the comprehensive new CMIP5 data set is available. For example, for monotonically increasing forcing paths, global transient temperature changes linearly with the forcing[23,28] or, alternatively, with the global transient climate response determined from AOGCMs or observations[29]. The ratio between the temperature increase by the end of the twenty-first century and the net anthropogenic radiative forcing shows little variation in our projections, except for RCP3-PD. For all monotonically increasing forcing scenarios that we analyse, this ratio has a mean value in 2100 of 0.62 °C $(W\,m^{-2})^{-1}$ with a standard deviation of 0.03. For RCP3-PD, the only scenario with a peak and decline evolution of its radiative forcing, this ratio becomes 0.88 °C $(W\,m^{-2})^{-1}$, which indicates that by 2100 RCP3-PD is closer to or even above the equilibrium warming that corresponds to its 2100 forcing.

With the probabilistic projections of this study, a consistent comparison between SRES scenarios and RCPs is established. A direct comparison, by either computing the new RCPs with old AOGCM versions or computing at least one of the SRES scenarios with the new model versions, could yield even more insights. Therefore, the inclusion of one of the SRES scenarios (for example, SRES A1B) in the set of scenarios ran by the CMIP5 models would be advantageous. Such an inclusion would greatly facilitate determining whether differences between CMIP3 and CMIP5 AOGCM results are due to the new scenarios or due to updated model versions.

Methods

Climate sensitivity characterizes the global surface temperature response on timescales of several centuries and includes the feedbacks due to water vapour, lapse rate, clouds and surface albedo, that is, the feedbacks that scale with temperature and that are implemented in CMIP3-type models. Feedbacks that have their own intrinsic long timescale (slow vegetation changes or ice sheets) are not considered and would enhance this concept to what is often called 'Earth system sensitivity' (see ref. 11).

In this study we define an average ECS PDF that is consistent with the overall consensus understanding of ECS of the IPCC AR4. We create ten thousand ECS distributions by spline interpolation between uniform sampled constraints based on the uncertainty ranges defined in the IPCC AR4. A total of eight constraints are sampled that define six points of a cumulative PDF (Fig. 1 and Supplementary Table S1): the temperature at the starting point, the cumulative probability at respectively 1.5 °C, 2 °C, 4.5 °C and at the point of inflection, the temperature at the point of inflection, the slope at the point of inflection and the temperature at the end point. These constraints are sampled randomly from uniformly distributed ranges that are chosen in a way such that they do not infer additional constraints beyond the synthesizing statements of the IPCC AR4 but, on the contrary, facilitate an as broad sampling of the remaining space as possible (see Supplementary Fig. S3). Each set of eight parameters yields a cumulative ECS distribution by applying a cubic spline interpolation through the six points the parameters define. Subsequently, each cumulative sensitivity distribution is tested for validity. For example, there is no evidence in the literature that supports multi-modal distributions of ECS (ref. 11). For each distribution, we check that: the cumulative probability between 2 °C and 4.5 °C is at least 66%, only one maximum (peak) is present, the cumulative PDF increases monotonically (this implies that the cumulative PDF does not undershoot zero probability and does not overshoot 100% probability), and no sudden changes in the first derivative of the PDF are allowed (that is, the distribution is kept relatively smooth by limiting the curvature outside a 1 °C range around the peak to a maximum value). Finally, our

© 2012 Macmillan Publishers Limited. All rights reserved.

representative ECS distribution is computed by taking the arithmetic mean over all ten thousand randomly drawn distributions.

ECS is not the only source of uncertainty for projecting transient global-mean temperatures for specific emission scenarios that is taken into account in our set-up of the MAGICC model. From a large 82-dimensional joint distribution of climate and radiative forcing parameters affecting the transient climate response, we draw our parameter sets such that the marginal ECS matches a specific distribution[10]. When deriving this joint distribution, we applied year 2005 uncertainty distributions for radiative forcings as prior distributions following Table 2.12 in ref. 30 and used observed hemispheric land/ocean temperatures[8] and ocean heat uptake[9] as historical constraints, as described previously[10]. In addition to the historically constrained climate response parameters, we reflect uncertainties in future carbon-cycle responses by using—at random—one of nine C^4MIP carbon-cycle model emulations. These emulations with MAGICC closely reflect the carbon pool dynamics when taking into account C^4MIP carbon-cycle climate[6]. In earlier set-ups[31,32], a specific ECS distribution from the literature was matched[10]. Here we apply the same methodology to match the ECS distribution described in this study.

Whereas the SRES scenarios provide GHG emissions pathways, the RCPs are GHG concentration pathways. In our set-up, we use the GHG emissions pathways as provided in ref. 2, and the concentration pathways described in ref. 25, as recommended for CMIP5. We also provide results for emission-driven RCP runs in Supplementary Table S3.

Temperature projections 'relative to pre-industrial' are calculated relative to the 1850 to 1875 base period.

Received 26 August 2011; accepted 22 December 2011; published online 5 February 2012

References

1. IPCC *Climate Change 2007: The Physical Science Basis* (eds Solomon, S. et al.) (Cambridge Univ. Press, 2007).
2. IPCC *Special Report on Emissions Scenarios* (eds Nakicenovic, N. & Swart, R.) (Cambridge Univ. Press, 2000).
3. Meehl, G. A., Covey, C., McAvaney, B., Latif, M. & Stouffer, R. J. Overview of the coupled model intercomparison project. *Bull. Am. Meteorol. Soc.* **86,** 89–93 (2005).
4. Moss, R. H. *et al.* The next generation of scenarios for climate change research and assessment. *Nature* **463,** 747–756 (2010).
5. Taylor, K. E., Stouffer, R. J. & Meehl, G. A. *A Summary of the CMIP5 Experiment Design* (Program for Climate Model Diagnosis and Intercomparison (PCMDI), 2011); available at http://cmip-pcmdi.llnl.gov/cmip5/docs/Taylor_CMIP5_design.pdf.
6. Meinshausen, M., Raper, S. C. B. & Wigley, T. M. L. Emulating coupled atmosphere–ocean and carbon cycle models with a simpler model, MAGICC6 – Part 1: Model description and calibration. *Atmos. Chem. Phys.* **11,** 1417–1456 (2011).
7. Meinshausen, M., Wigley, T. M. L. & Raper, S. C. B. Emulating atmosphere–ocean and carbon cycle models with a simpler model, MAGICC6 – Part 2: Applications. *Atmos. Chem. Phys.* **11,** 1457–1471 (2011).
8. Brohan, P., Kennedy, J. J., Harris, I., Tett, S. F. B. & Jones, P. D. Uncertainty estimates in regional and global observed temperature changes: A new data set from 1850. *J. Geophys. Res.* **111,** D12106 (2006).
9. Domingues, C. M. *et al.* Improved estimates of upper-ocean warming and multi-decadal sea-level rise. *Nature* **453,** 1090–U1096 (2008).
10. Meinshausen, M. *et al.* Greenhouse-gas emission targets for limiting global warming to 2 °C. *Nature* **458,** 1158–1162 (2009).
11. Knutti, R. & Hegerl, G. C. The equilibrium sensitivity of the Earth's temperature to radiation changes. *Nature Geosci.* **1,** 735–743 (2008).
12. IPCC *Guidance Notes for Lead Authors of the IPCC Fourth Assessment Report on Addressing Uncertainties* 5 (2005); available at http://www.ipcc.ch/pdf/supporting-material/uncertainty-guidance-note.pdf.
13. Roe, G. H. & Baker, M. B. Why is climate sensitivity so unpredictable? *Science* **318,** 629–632 (2007).
14. Tomassini, L., Reichert, P., Knutti, R., Stocker, T. F. & Borsuk, M. E. Robust Bayesian uncertainty analysis of climate system properties using Markov chain Monte Carlo methods. *J. Clim.* **20,** 1239–1254 (2007).
15. Royer, D. L., Berner, R. A. & Park, J. Climate sensitivity constrained by CO_2 concentrations over the past 420 million years. *Nature* **446,** 530–532 (2007).
16. Mastrandrea, M. D. *et al. Guidance Notes for Lead Authors of the IPCC Fifth Assessment Report on Consistent Treatment of Uncertainties* 5 (2010); available at http://www.ipcc.ch/pdf/supporting-material/uncertainty-guidance-note.pdf.
17. Socolow, R. High-consequence outcomes and internal disagreements: Tell us more, please. *Climatic Change* **108,** 775–790 (2011).
18. Wigley, T. M. L. & Raper, S. C. B. Interpretation of high projections for global-mean warming. *Science* **293,** 451–454 (2001).
19. Knutti, R., Joos, F., Müller, S. A., Plattner, G-K. & Stocker, T. F. Probabilistic climate change projections for CO_2 stabilization profiles. *Geophys. Res. Lett.* **32,** L20707 (2005).
20. Meinshausen, M. in *Avoiding Dangerous Climate Change* (eds Schellnhuber, J. S. *et al.*) (Cambridge Univ. Press, 2006).
21. Meehl, G. A. *et al.* in *IPCC Climate Change 2007: The Physical Science Basis* (eds Solomon, S. *et al.*) (Cambridge Univ. Press, 2007).
22. UNFCCC *FCCC/CP/2010/7/Add.1 Decision 1/CP.16 31* (UNFCCC, 2010).
23. Knutti, R. *et al.* A review of uncertainties in global temperature projections over the twenty-first century. *J. Clim.* **21,** 2651–2663 (2008).
24. Tebaldi, C. & Knutti, R. The use of the multi-model ensemble in probabilistic climate projections. *Phil. Trans. R. Soc. A* **365,** 2053–2075 (2007).
25. Meinshausen, M. *et al.* The RCP greenhouse gas concentrations and their extensions from 1765 to 2300. *Climatic Change* **109,** 213–241 (2011).
26. van Vuuren, D. P. *et al.* Stabilizing greenhouse gas concentrations at low levels: An assessment of reduction strategies and costs. *Climatic Change* **81,** 119–159 (2007).
27. Riahi, K., Gruebler, A. & Nakicenovic, N. Scenarios of long-term socio-economic and environmental development under climate stabilization. *Technol. Forecasting Soc. Change (Special Issue: Greenhouse Gases—Integrated Assessment)* **74,** 887–935 (2007).
28. Gregory, J. M. & Forster, P. M. Transient climate response estimated from radiative forcing and observed temperature change. *J. Geophys. Res.* **113,** D23105 (2008).
29. Knutti, R. & Tomassini, L. Constraints on the transient climate response from observed global temperature and ocean heat uptake. *Geophys. Res. Lett.* **35,** L09701 (2008).
30. Forster, P. *et al.* in *IPCC Climate Change 2007: The Physical Science Basis* (eds Solomon, S. *et al.*) 129–234 (Cambridge Univ. Press, 2007).
31. UNEP *The Emissions Gap Report—Are the Copenhagen Accord Pledges Sufficient to Limit Global Warming to 2 °C or 1.5 °C*? (UNEP, 2010).
32. Rogelj, J. *et al.* Copenhagen Accord pledges are paltry. *Nature* **464,** 1126–1128 (2010).
33. Hegerl, G. C., Crowley, T. J., Hyde, W. T. & Frame, D. J. Climate sensitivity constrained by temperature reconstructions over the past seven centuries. *Nature* **440,** 1029–1032 (2006).
34. Forster, P. M. D. & Gregory, J. M. The climate sensitivity and its components diagnosed from Earth radiation budget data. *J. Clim.* **19,** 39–52 (2006).
35. Annan, J. D. & Hargreaves, J. C. Using multiple observationally-based constraints to estimate climate sensitivity. *Geophys. Res. Lett.* **33,** L06704 (2006).
36. Forest, C. E., Stone, P. H. & Sokolov, A. P. Estimated PDFs of climate system properties including natural and anthropogenic forcings. *Geophys. Res. Lett.* **33,** L01705 (2006).
37. Knutti, R., Meehl, G. A., Allen, M. R. & Stainforth, D. A. Constraining climate sensitivity from the seasonal cycle in surface temperature. *J. Clim.* **19,** 4224–4233 (2006).
38. Murphy, J. M. *et al.* Quantification of modelling uncertainties in a large ensemble of climate change simulations. *Nature* **430,** 768–772 (2004).
39. Piani, C., Frame, D. J., Stainforth, D. A. & Allen, M. R. Constraints on climate change from a multi-thousand member ensemble of simulations. *Geophy. Res. Lett.* **32,** L23825 (2005).
40. Frame, D. J., Stone, D. A., Stott, P. A. & Allen, M. R. Alternatives to stabilization scenarios. *Geophys. Res. Lett.* **33,** L14707 (2006).
41. IPCC *Scientific Assessment of Climate Change: Report of Working Group I* (eds Houghton, J. T., Jenkins, G. J. & Ephraums, J . J.) (Cambridge Univ. Press, 1990).
42. IPCC *Climate Change 1995: The Science of Climate Change 572* (eds Houghton. J. T. et al.) (Cambridge Univ. Press, 1996).
43. IPCC *Climate Change 2001: The Scientific Basis* (eds Houghton. J. T. et al.) (Cambridge Univ. Press, 2001).
44. Frame, D. J. *et al.* Constraining climate forecasts: The role of prior assumptions. *Geophys. Res. Lett.* **32,** L09702 (2005).
45. Andronova, N. G. & Schlesinger, M. E. Objective estimation of the probability density function for climate sensitivity. *J. Geophys. Res. Atmos.* **106,** 22605–22611 (2001).
46. Forest, C. E., Stone, P. H., Sokolov, A., Allen, M. R. & Webster, M. D. Quantifying uncertainties in climate system properties with the use of recent climate observations. *Science* **295,** 113–117 (2002).
47. Gregory, J. M., Stouffer, R. J., Raper, S. C. B., Stott, P. A. & Rayner, N. A. An observationally based estimate of the climate sensitivity. *J. Clim.* **15,** 3117–3121 (2002).
48. Knutti, R., Stocker, T. F., Joos, F. & Plattner, G. K. Constraints on radiative forcing and future climate change from observations and climate model ensembles. *Nature* **416,** 719–723 (2002).

Acknowledgements

J.R. was supported by the Swiss National Science Foundation (project 200021-135067).

Author contributions

All authors were involved in designing the research; M.M. developed the set-up of the MAGICC model; J.R. developed the climate sensitivity sampling methodology and carried out the analysis; all authors contributed to writing the paper.

Additional information

The authors declare no competing financial interests. Supplementary information accompanies this paper on www.nature.com/natureclimatechange. Reprints and permissions information is available online at www.nature.com/reprints. Correspondence and requests for materials should be addressed to J.R.

© 2012 Macmillan Publishers Limited. All rights reserved.